Aromatic π-Stacking in Solution as Revealed through the Aggregation of Phenylacetylene Macrocycles

Ashok S. Shetty, Jinshan Zhang,† and Jeffrey S. Moore*

Contribution from the Departments of Chemistry and Materials Science & Engineering and The Beckman Institute for Advanced Science and Technology, University of Illinois, Urbana, Illinois 61801

Received August 21, 1995[⊗]

Abstract: Aggregation of phenylacetylene macrocycles (PAMs) in solution has been studied by ^{1}H NMR spectroscopy and vapor pressure osmometry. The association constant for dimerization, K_{assoc}, has been determined by curve fitting the concentration dependence of ^{1}H NMR chemical shifts to a model for monomer−dimer equilibrium. The reliability of the NMR-determined aggregation constants and aggregate size have been independently verified by vapor pressure osmometry measurements. Thermodynamic parameters for association have been obtained from van't Hoff analyses which show the aggregation to be favored enthalpically. The aggregation of PAMs bearing various *endo*- and *exo*-annular functional groups and PAMs of different geometry and ring size has been studied. The type of pendant functional groups and the manner in which these groups are arranged on the macrocycle is shown to strongly influence self-association. PAMs substituted with electron withdrawing groups (e.g., esters) are more strongly associated than those bearing electron donating groups (e.g., alkyl ethers) or macrocycles bearing a combination of the two substituents. The type of alkyl substituent on the ester or ether group is less important as long as the substituent is not branched and is *exo*-annular. *Endo*-annular alkyl ethers as well as branched *exo*-annular alkyl esters severely disrupt aggregation. Rigidity of the macrocycle also influences self-association. In contrast to hexameric macrocycles, similarly substituted open-chain oligomers and a nonplanar macrocycle show much weaker association. These findings are discussed in the context of face-to-face $\pi-\pi$ interactions between aromatic rings. Consideration has also been given to $\pi-\pi$ interactions between aromatic and ethynyl groups and between a pair of acetylenes, but these are concluded to be less significant based on an analysis of data from the Cambridge Structural Database.

Introduction

Interactions between aromatic units play a significant role in supramolecular chemistry. It has been well documented that aryl groups prefer to associate in either an edge-to-face or an offset, face-to-face orientation.[1] Examples illustrating the importance and diversity of these interactions include the vertical base pair association that stabilizes the double helical structure of DNA,[2] intercalation of small molecules between nucleotides,[3] packing of aromatic molecules in crystals,[4] the tertiary structures of proteins,[1b] host−guest binding,[5] and aggregation of porphyrins in solution.[6] Offset, face-to-face π-stacking interactions have been the subject of a number of investigations.[7] These studies have addressed the role of molecular geometry[4a,8] and electrostatic factors in promoting aromatic association.[7g,9−11] Desiraju and Gavezzotti proposed that the packing of polyaromatic hydrocarbons in solids is dictated by the molecular shape.[4a,8] Their model does correlate molecular shape and packing mode for a number of polyaromatic hydrocarbons, but it does not take into consideration the electronic factors due to substituents, which are also known to be important.

* Author to whom correspondence should be addressed.

† Current address: Motorola Inc., 1750 Belle Meade Court, Lawrenceville, GA 30243.

⊗ Abstract published in *Advance ACS Abstracts,* January 15, 1996.

(1) (a) Burley, S. K.; Petsko, G. A. *Adv. Protein. Chem.* **1988**, *39*, 125. (b) Hunter, C. A.; Singh, J.; Thornton, J. M. *J. Mol. Biol.* **1991**, *218*, 837.

(2) Saenger, W. *Principles of Nucleic Acid Structure*; Springer-Verlag: New York, 1984; pp 132−140.

(3) Wakelin, L. P. G. *Med. Res. Rev.* **1986**, *6*, 275.

(4) (a) Desiraju, G. R.; Gavezzotti, A. *J. Chem. Soc., Chem. Commun.* **1989**, 621. (b) Desiraju, G. R. *Crystal Engineering: The Design of Organic Solids*, Elsevier, New York, 1989. (c) Holligan, B. M.; Jeffrey, J. C.; Ward, M. D. *J. Chem. Soc., Dalton Trans*. **1992**, *23*, 3337. (d) Carter, P. W.; Dimagno, S. G.; Porter, J. D.; Streitwieser, A. *J. Phys. Chem*. **1993**, *97*, 1085. (e) Grubbs, R. H.; Kratz, D. *Chem. Ber*. **1993**, *126*, 149. (f) Flock, M.; Nieger, M.; Breitmaier, E. *Liebigs Ann. Chem.* **1993**, *4*, 451. (g) Takimiya, K.; Ohnishi, A.; Aso, Y.; Otsubo. T.; Ogura, F.; Kawabata. K.; Tanaka. K.; Mizutani. M. *Bull. Chem. Soc. Jpn.* **1994**, *67*, 766. (h) Miyamura, K.; Mihara, A.; Fujii, T.; Gohshi, Y.; Ishii, Y. *J. Am. Chem. Soc*. **1995**, *117*, 2377.

(5) (a) Benzing, T.; Tjivikua, T.; Wolfe, J.; Rebek, J., Jr. *Science* **1988**, *242*, 266. (b) Cram, D. J. *Angew. Chem., Int. Ed. Engl.* **1988**, *27*, 1009. (c) Muehldorf, A. V.; Van Engen, D.; Warner, J. C.; Hamilton, A. D. *J. Am. Chem. Soc.* **1988,** *110*, 6561. (d) Zimmerman, S. C.; Wu, W. *J. Am. Chem. Soc.* **1989**, *111*, 8054. (e) Pirkle, W. H.; Burke, J. A.; Wilson, S. R. *J. Am. Chem. Soc*. **1989**, *111*, 9222. (f) Cochran, J. E.; Parrott, T. J.; Whitlock, B. J.; Whitlock, H. W. *J. Am. Chem. Soc.* **1992**, *114*, 2269. (g) Suzuki, M.; Ohmor, H.; Kajtar, M.; Szejtli, J.; Vikmon, M. *J. Incl. Phen. Mol. Rec*. **1994**, *18*, 255. (h) Pirkle, W. H.; Selness, S. R. *J. Org. Chem*. **1995**, *60*, 3252.

(6) (a) Alexander, A. E. *J. Chem. Soc.* **1937**, 1813. (b) Hughes, A. *Proc. R. Soc. London, Ser. A* **1936**, *155*, 710. (c) Abraham, R. J.; Eivazi, F.; Pearson, H.; Smith, K. M. *J. Chem. Soc., Chem. Commun.* **1976**, 698. (d) White, W. In *The Porphyrins*; Dolphin, D., Ed.; Academic Press: New York, 1978, Vol. V, Chapter 7. (e) Schneider, H. J.; Wang, M. *J. Org. Chem*. **1994**, *59*, 7464. (f) Miura, M.; Majumder, S. A.; Hobbs, J. D.; Renner, M. W.; Furenlid, L. R. Shelnutt, J. A. *Inorg. Chem*. **1994**, *33*, 6078.

(7) For general references, see: (a) Tucker, E. E.; Christian, S. D. *J. Phys. Chem*. **1979**, *83*, 426. (b) Ravishanker, G.; Beverridge, D. L. *J. Am. Chem. Soc*. **1985**, *107*, 2565. (c) Jorgensen, W. L.; Severance, D. L. *J. Am. Chem. Soc*. **1990**, *112*, 4768. (d) Tucker, J. A.; Houk, K. N.; Trost, B. M. *J. Am. Chem. Soc*. **1990**, *112*, 5465. (e) Linse, P. *J. Am. Chem. Soc.* **1992**, *114*, 4366. (f) Leighton, P.; Cowan, J. A.; Abraham, R. J.; Sanders, J. K. M. *J. Org. Chem*, **1988**, *53*, 733. (g) Hunter, C. A.; Sanders, J. K. M. *J. Am. Chem. Soc.* **1990**, *112*, 5525. (h) Hunter, C. A.; Meah, M. N.; Sanders, J. K. M. *J. Am. Chem. Soc.* **1990**, *112*, 5773. (i) Anderson, H. L.; Hunter, C. A.; Meah, M. N.; Sanders, J. K. M. *J. Am. Chem. Soc*. **1990**, *112*, 5780. (j) Hunter, C. A. *Chem. Soc. Rev*. **1994**, *23*, 101. (k) Duffy, E. M.; Jorgensen, W. L. *J. Am. Chem. Soc*. **1994**, *116*, 6337. (l) Kurita, Y.; Takayama, C.; Tanaka, S. *J. Comp. Chem*. **1995**, *16*, 131. (m) Laatikainen, R.; Ratilainen, J.; Sebastian, R.; Santa, H. *J. Am. Chem. Soc.* **1995**, *117*, 11006.

(8) Desiraju, G. R.; Gavezzotti, A. *Acta Crystallogr*. **1989**, *B45*, 473.

0002-7863/96/1518-1019$12.00/0

Substituents strongly influence face-to-face stacking tendencies, though these effects cannot always be explained in terms of intuitive donor−acceptor concepts. This is illustrated by the surprisingly high association constant of complexes of 1,3,5-trinitrobenzene with aromatic substrates having strong electron withdrawing groups.[9] Donor−acceptor concepts also fail to explain why aromatic hydrocarbons associate strongly with aromatic fluorocarbons in a face-to-face orientation. For example, in the binary complex between benzene and hexafluorobenzene (HFB), spectroscopic data provide no appreciable evidence of intermolecular charge transfer.[12] These examples point to the conclusion that intermolecular interactions other than charge transfer must contribute significantly to face-to-face stabilization. Over the past two decades, evidence has accumulated which provides a consistent model emphasizing the role of other electrostatic forces in stabilizing or destabilizing aromatic face-to-face stacking. In 1974, Brown and Swinton demonstrated that the stability of the benzene−HFB complex can be explained by quadrupole−quadrupole interactions rather than charge-transfer interactions.[11b] This has recently been quantified by Williams in a detailed analysis of the origin of the phase transition seen in the benzene−HFB complex.[13]

Lately, electrostatic concepts have been recast into more pragmatic models to provide chemically intuitive pictures of how electronic factors can influence aromatic π-stacking. In 1990, Hunter and Sanders introduced a model which illustrated how the spatial distribution of charge imposed by the aromatic geometry and its pendant substituents can account for face-to-face and edge-to-face preferences.[7g] Cozzi and Siegel have introduced the term "polar/π" to emphasize that aromatic interactions are largely the result of electrostatics and that the aromatic ring, including benzene, possesses a distinctly polar character.[14]

The interaction energies involved in aromatic association are small, making it especially difficult to study this phenomenon in solution. Therefore, molecules in which these interactions are amplified may be valuable for studying aromatic π-stacking. Here we report in detail the self-association of phenylacetylene macrocycles (PAMs) in solution.[15] These macrocycles can be viewed as a collection of aromatic rings held in a rigid framework which permit association phenomena to be studied even though the pairwise interaction between individual aromatic units is weak. PAMs are prepared by the cyclization of sequence-specific phenylacetylene oligomers. Combinations of ortho-, meta-, and para-substituted phenylacetylene monomers can give essentially any cyclic framework consistent with polygons of the trigonal lattice.[16] The size of the macrocyclic ring is governed by the number of monomer units in the sequence, while the placement of the functional groups on the PAM is dependent on the comonomer order in the precursor sequence. Therefore PAMs can be both site-specifically functionalized and adopt a variety of geometries (Charts 1 and 2).[17] The synthetic diversity available with this chemistry makes PAMs a suitable system for investigating aromatic interactions in solution through studies of their self-association. The information gained from these studies will not only provide insight into the nature of these interactions but will also contribute to the understanding of their supramolecular organization, which is important for the development of tubular mesophases,[18] porous organic solids,[19] and organic monolayers[20] based on PAM building blocks.

Chart 1

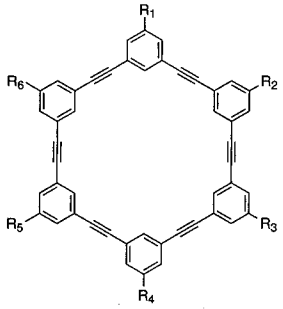

1: $R_1 = R_2 = R_3 = R_4 = R_5 = R_6 = COO^nC_4H_9$
2: $R_1 = R_2 = R_3 = R_4 = R_5 = R_6 = OCO^nC_4H_9$
3: $R_1 = R_2 = R_3 = R_4 = R_5 = R_6 = COO^nC_7H_{15}$
4: $R_1 = R_2 = R_3 = R_4 = R_5 = R_6 = COO^nC_8H_{17}$
5: $R_1 = R_2 = R_3 = R_4 = R_5 = R_6 = COO^nC_{16}H_{33}$
6: $R_1 = R_2 = R_3 = R_4 = R_5 = R_6 = COO^tC_4H_9$
7: $R_1 = R_2 = R_3 = R_4 = R_5 = R_6 = CH_2O^nC_4H_9$
8: $R_1 = R_2 = R_3 = R_4 = R_5 = R_6 = O^nC_4H_9$
9: $R_1 = R_2 = R_3 = R_4 = R_5 = R_6 = O^nC_6H_{13}$
10: $R_1 = R_2 = R_3 = R_4 = R_5 = R_6 = O^nC_7H_{15}$
11: $R_1 = R_2 = R_3 = R_4 = R_5 = R_6 = O^nC_8H_{17}$
12: $R_1 = R_2 = R_3 = R_4 = R_5 = R_6 = O^nC_{10}H_{21}$
13: $R_1 = R_3 = R_5 = COO^nC_4H_9$, $R_2 = R_4 = R_6 = O^nC_4H_9$
14: $R_1 = R_2 = R_3 = COO^nC_4H_9$, $R_4 = R_5 = R_6 = O^nC_4H_9$

Results

Qualitative NMR Observations. It became evident during routine examination of the ^{1}H NMR spectrum of **1** that the aromatic chemical shifts of this macrocycle were very dependent on concentration.[15] At ambient temperature, the chemical shifts in $CDCl_3$ of the two anisochronous aromatic protons varied from δ 8.12 to 7.23 and from δ 7.81 to 6.89 as the concentration changed from 0.83 to 106 mM (Figure 1). The chemical shifts of the aliphatic protons, unlike those of the aromatic protons, remained relatively unchanged over the same concentration range. In addition, no evidence of chemical shift changes of the aromatic protons were observed in benzene-d_6. In contrast to the ^{1}H NMR data in $CDCl_3$, the ^{13}C NMR chemical shifts were less sensitive to changes in concentration (Figure 2).

These observations suggest that **1** self-associates in chloroform solution. To gain insight into the nature of this aggregation phenomenon, we decided to further investigate the solution behavior of PAMs by systematically varying their size, electronic nature, and the orientation of their substituents (Charts 1 and 2). Contrary to **1**, the chemical shifts of the aromatic protons in **2** remained essentially constant over a large concentration range. The only difference between these isomeric PAMs is the mode of substituent linkage. In **1**, the carbonyl groups are directly attached to the phenyl rings, while in **2**, they are linked through oxygen atoms. In addition, PAMs with

(9) Foster, R. *Organic Charge-Transfer Complexes*; Academic Press: London, 1969; p 197.
(10) Muehldorf, A. V.; Van Engen, D.; Warner, J. C.; Hamilton, A. D. *J. Am. Chem. Soc.* **1988**, *110*, 6561.
(11) (a) Hobza, P.; Selzle, H. L.; Schlag, E. W. *J. Am. Chem. Soc.* **1994**, *116*, 3500. (b) Brown, N. M. D.; Swinton, F. L. *J. Chem. Soc., Chem. Commun.* **1974**, 770. (c) Hernández-Trujillo, J.; Costas, M.; Vela, A. *J. Chem. Soc., Faraday Trans.* **1993**, *89(14)*, 2441. (d) Williams, J. H. *Acc. Chem. Res.* **1993**, *26*, 593. (e) Luhmer, M.; Bartik, K.; Dejaegere, A.; Bovy, P.; Reisse, J. *Bull. Soc. Chim. Fr.* **1994**, *131*, 603.
(12) Williams, J. H. *Chem. Phys.* **1992**, *167*, 215.
(13) Williams, J. H. *Chem. Phys.* **1993**, *172*, 171.
(14) Cozzi, F.; Siegel, J. S. *Pure Appl. Chem.* **1995**, *67*, 683.
(15) For a preliminary account of this study, see: Zhang, J.; Moore, J. S. *J. Am. Chem. Soc.* **1992**, *114*, 9701.
(16) Young, J. K.; Moore, J. S. In *Modern Acetylene Chemistry*; Stang, P., Diederich, F., Eds.; VCH Publications: Weinheim, 1995; pp 415−442.
(17) Zhang, J.; Pesak, D. J.; Ludwick, J. J.; Moore, J. S. *J. Am. Chem. Soc.* **1994**, *116*, 4227.
(18) Zhang, J.; Moore, J. S. *J. Am. Chem. Soc.* **1994**, *116*, 2655.
(19) Venkataraman, D.; Lee, S.; Zhang, J.; Moore, J. S. *Nature* **1994**, *371*, 591.
(20) Shetty, A. S.; Stork, K. F.; Bohn, P. W.; Moore, J. S. Manuscript in preparation.

Chart 2

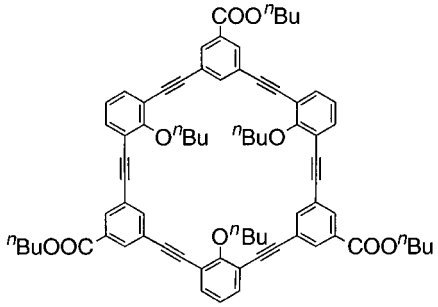

15

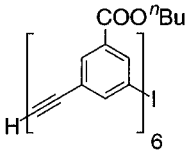

16

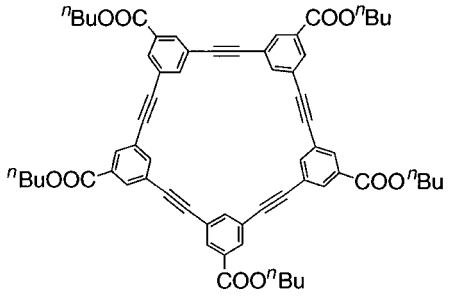

17

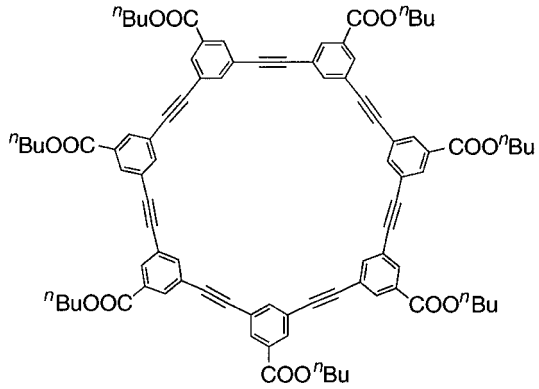

18

electron donating groups, such as **7**−**12**, showed no concentration dependent chemical shift changes even at temperatures as low as 223 K. PAMs **13** and **14**, having an equal number of ester and ether groups, exhibited chemical shift changes as a function of concentration, but the magnitude of these changes was smaller than **1**. These observations suggest that the association is sensitive to the electronic factors of the substituents.

To investigate hetero-association between donor and acceptor macrocycles, mixtures of **1** and **7** as well as **1** and **8** were studied by ^{1}H NMR titration.[21] The chemical shifts of **1** as well as the aromatic protons of **7** (or **8**) changed as the concentration of **1** increased. However, the change observed for **7** (or **8**) was less than that observed for **1** in this mixture over the same concentration range. Clearly these titration experiments are complicated by competition between self-association of **1** and hetero-association between **1** and **7** (or **8**).

For PAMs containing ester substituents, the concentration dependent chemical shift changes were insensitive to the type

(21) Wilcox, C. S. in *Frontiers in Supramolecular Organic Chemistry and Photochemistry;* Schneider, H.-J.; Durr, H., Eds.; VCH: New York, 1991, pp 123−143.

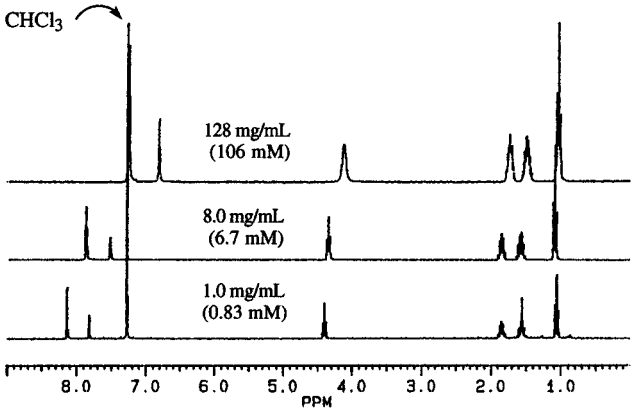

Figure 1. Concentration dependence of ^{1}H NMR spectra (360 MHz) of **1** in $CDCl_3$ at room temperature.

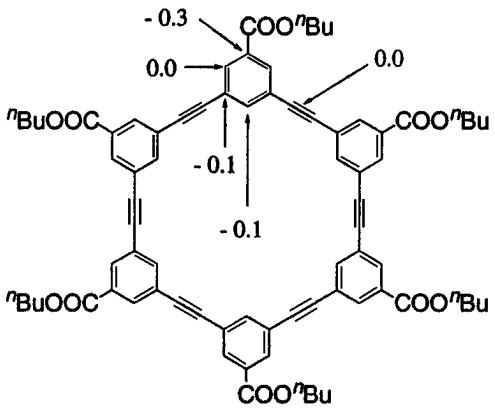

Figure 2. ^{13}C NMR (90 MHz) chemical shift differences ($\Delta\ \delta$) of various carbon nuclei of **1** upon changing the concentration from 26 to 53.3 mM at ambient temperature in $CDCl_3$.

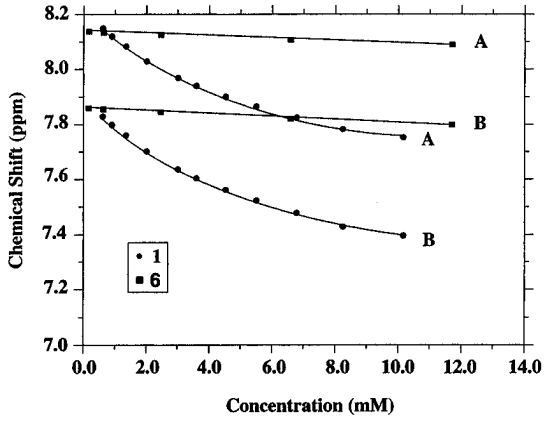

Figure 3. Concentration dependence of ^{1}H NMR chemical shifts for aromatic protons of **1** and **6** (in $CDCl_3$ at ambient temperature). The curves marked **A** and **B** are for the *exo*-annular and the *endo*-annular protons, respectively.

of alkyl groups employed, provided they were unbranched. For example, over the same concentration range, PAMs **3**−**5** containing ester groups of varying chain lengths showed chemical shift changes very similar to those of **1**. On the other hand, PAM **6**, functionalized with *tert*-butyl ester groups, showed no significant chemical shift dependence on concentration (Figure 3). These observations indicated that slight modifications to the steric environment in the vicinity of the aromatic framework significantly alters the solution aggregation behavior of PAMs.

Besides the steric and electronic factors, it was found that the concentration dependence of chemical shifts varied according to how the substituents were arranged around the macrocyclic

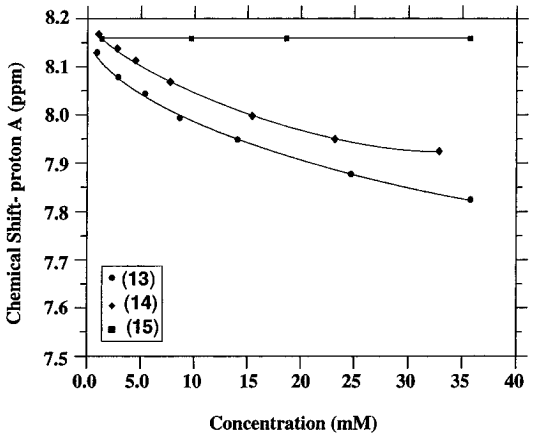

Figure 4. Concentration dependence of ^{1}H NMR chemical shift for the *exo*-annular proton, of the aromatic ring with the ester substituent, of **13**, **14**, and **15** (in $CDCl_3$ at ambient temperature).

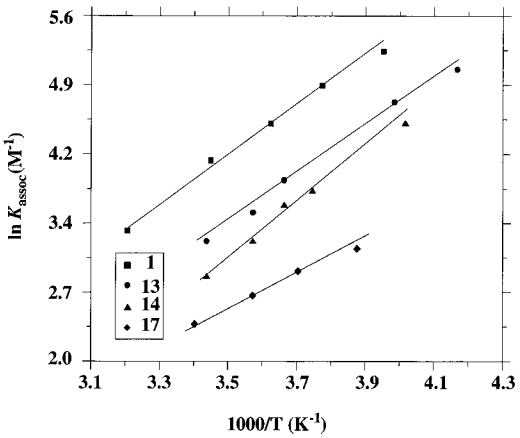

Figure 5. van't Hoff plots of self-association constants (K_{assoc}) for PAMs **1**, **13**, **14**, and **17** in $CDCl_3$.

skeleton. This is revealed by constitutional isomers **13**−**15**. Though PAMs **13**−**15** all have an equal number of ester and ether groups, the magnitude of their chemical shift changes varied considerably. As shown in Figure 4, PAM **15** showed no concentration dependent chemical shift changes while in the same concentration range, PAMs **13** and **14** had a chemical shift difference of δ 0.31 and δ 0.24, respectively. In **15** the ether groups are *endo*-annular, while **13** and **14** have *exo*-annular substituents, but they differ in the order of these groups around the macrocycle.

The rigidity and geometry of the PAMs also had a strong influence upon the magnitude of the concentration dependent changes in ^{1}H NMR shifts. This is evident because the ^{1}H NMR of **16**, the linear chain precursor to **1**, revealed no chemical shift changes as a function of concentration. PAMs **17** and **18**, with five and seven phenylacetylene subunits, respectively, showed smaller chemical shift changes than PAM **1**.

Quantitative Interpretation of the ^{1}H NMR Data. A single PAM molecule (i.e., monomeric species, M) can be considered to aggregate as follows

$$M \underset{+M}{\overset{-M}{\rightleftharpoons}} M_2 \underset{+M}{\overset{-M}{\rightleftharpoons}} M_3 \underset{+M}{\overset{-M}{\rightleftharpoons}} \ldots \quad (1)$$

If we assume that the monomer−dimer equilibrium is the predominant process, the ^{1}H NMR chemical shifts at different concentrations can be used to determine the dimerization constant, K_{assoc}, using curve fitting methods described in the Appendix. Implicit in this assumption is that higher order aggregation beyond dimerization is insignificant in the concentration range studied. Clearly at higher concentrations larger aggregates may become more significant.[22] Saunder−Hyne analysis of our NMR data for **1** shows that the monomer−dimer model gives the best fit over the concentration range we have studied. This was further confirmed by the VPO measurements described below. From determination of K_{assoc} as a function of temperature, van't Hoff analyses were performed to obtain thermodynamic quantities for the aggregation of PAMs. The van't Hoff plots for PAMs **1**, **13**, **14**, and **17** are shown in Figure 5 while the values for ΔH and ΔS are given in Table 1. The signs of ΔS and ΔH suggest that the aggregation of PAMs in solution is not an entropically driven process but that it is slightly favored enthalpically.

Vapor Pressure Osmometry Measurements. Vapor pressure osmometry (VPO) was used to study the aggregate size as well as to independently verify the K_{assoc} values obtained from the above ^{1}H NMR observations. Osmotic measurements of the solutions of PAMs were conducted in chloroform at 308 K using benzil as a standard. The stoichiometric molal concentration was calculated from the weight of the solute, while the colligative molal concentration was obtained by comparing its VPO reading against that of benzil.[23] A plot of colligative concentration versus stoichiometric concentration for **3**, **6**, **15**, **16**, and **17** gave a straight line with a slope of unity and an intercept of almost zero indicating that these PAMs do not aggregate in chloroform solution. However, when the stoichiometric concentration of **1** was plotted against the colligative concentration, a nonlinear plot was found (Figure 6). The colligative concentration was lower than the stoichiometric concentration indicating that **1** self-associates in solution. Hence, the VPO results are, qualitatively, in agreement with the ^{1}H NMR observations. The VPO data can be interpreted quantitatively as outlined in the Appendix. This analysis reveals that higher order aggregation beyond the dimer is not significant for these compounds in the concentration range studied here. The dimerization constant determined from VPO is in very good agreement with the value obtained from the ^{1}H NMR study. The dimerization constant of **1**, in chloroform and at 308 K, was 40 and 35 M^{-1} by VPO and NMR, respectively.

Table 1. Thermodynamic Data for Self-Association of PAMs in $CDCl_3$

compd	K_{assoc} (M^{-1}) [a]	ΔG (kcal/mol)[a]	ΔH (kcal/mol)	ΔS (cal/mol·K)
1	60	−2.4	−5.0 ± 0.2	−9.2 ± 0.8
2	∼0			
6	∼0			
7	∼0			
8	∼0			
13	18	−1.7	−5.1 ± 0.3	−13.6 ± 1.0
14	26	−1.9	−5.6 ± 0.3	−10.8 ± 1.0
15	∼0			
17	11	−1.4	−3.3 ± 0.2	−6.6 ± 0.8
18	16	*b*	*b*	*b*

[a] At 293 K. [b] van't Hoff plot is not linear in the temperature range from 258 to 294 K.

Discussion

As **1** has no functional groups capable of hydrogen-bonding, it is believed that PAM association is the result of $\pi-\pi$ interactions. This is supported by the upfield shift of the aromatic protons due to the influence of the ring current from the neighboring molecule. This idea is further supported by the observation that only the aromatic protons show significant

(22) (a) Saunders, M.; Hyne, J. B. *J. Chem. Phys.* **1958**, *29*, 1319. (b) Marcus, S. H.; Miller, S. I. *J. Am. Chem. Soc.* **1966**, *88*, 3719. For fitting comparisions of our data to various models, see the supporting information.

(23) Schrier, E. E. *J. Chem. Educ.* **1968**, *45*, 176.

concentration-dependent chemical shifts. The chemical shifts of protons on the aliphatic substituents are almost invariant to concentration. Aromatic solvents are known to significantly reduce π-stacking interactions because the solvent molecules effectively solvate the solute.[24,25] The absence of concentration dependent chemical shift changes for **1** in benzene-d_6, thus, further supports a π-driven association.

Our experimental observations indicate that electron withdrawing substituents on the macrocycle favor self-association in comparison to electron donating substituents, as indicated by a comparison of the behavior of **1**, **2**, **7**, and **8**.[26] PAMs **1** and **2** are constitutional isomers in which the oxygen atom of **2** is directly linked to the phenyl rings as opposed to the carbonyl carbon as in **1**. Hence, the ester groups in **2** function as weak donors ($\sigma_p \approx 0.16$), while those in **1** are acceptors ($\sigma_p \approx 0.44$).[27] An attempt was made to study the hetero-association of **1** and **7** as well as **1** and **8** by NMR titration. Accurate values of these hetero-association constants could not be obtained due to the strong competition by self-association of **1**.

The self-association behavior of PAMs that have both electron withdrawing and electron donating groups is diminished relative to **1**. PAMs **13** and **14**, which are functionalized with ester and ether groups, have a K_{assoc} of 18 and 26 M^{-1} respectively, while **1** has a K_{assoc} of 60 M^{-1} (Table 1) at this same temperature. This is contrary to the intuitive notion that donor−acceptor interactions between the alkoxy and ester functionalities might favor aggregation. The values of ΔH and ΔS for PAM **13** suggest that donor−acceptor interactions between alkoxy and ester groups slightly favor π-stacking enthalpically but disfavor it entropically relative to **1**. Overall, the entropy effect dominates near ambient temperature, resulting in a decrease in K_{assoc} for **13**. The difference in ΔS values indicate that the dimer pair of **13** is more highly ordered than that of **1**. This could be due to the ordered sequence of substituents around the macrocyclic frame in **13** as compared to the highly symmetric structure of **1**.

The sensitivity of the PAM association process to the steric environment provides insight as to the geometry of the aggregates. While the length of the alkyl chains of the ester groups has no influence on the aggregation, branching of the alkyl groups in the vicinity of the aromatic core, affects it drastically. PAM **6**, with *tert*-butyl ester groups, shows no significant concentration dependent chemical shifts. The absence of self-association in this molecule was confirmed by VPO (Figure 6). It is presumed that the bulky *tert*-butyl groups prevent the PAMs from closely approaching each other, thereby hindering $\pi-\pi$ interactions. This observation suggests the notion that PAM aggregation involves a face-to-face stacking rather than an edge-to-face orientation. Additional details about the dimer geometry such as the extent of offset cannot be determined from the available information. The crystal structure of a related PAM molecule does however support the notion that the macrocycles stack in an offset face-to-face fashion.[19]

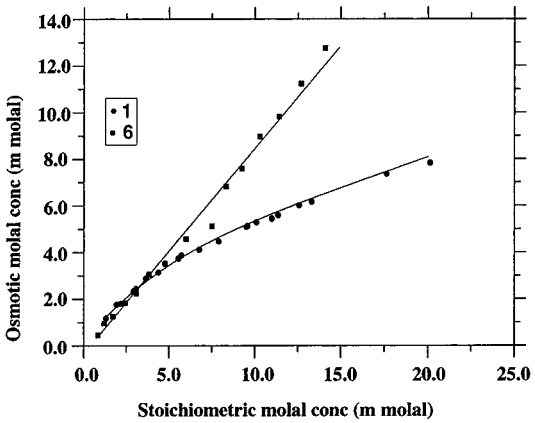

Figure 6. Colligative concentration obtained by VPO vs stoichiometric concentration for PAMs **1** and **6** in $CHCl_3$ at 308 K.

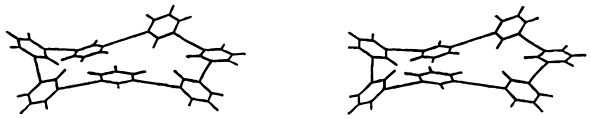

Figure 7. Stereoview of the carbon skeleton of PAM **18**. The conformation shown represents an energy minimum as determined by molecular mechanics using the QUANTA CHARMm force field.[28]

Another piece of evidence suggesting that PAMs associate via a face-to-face π-stacking interaction is obtained by comparing the concentration dependence of ^{1}H NMR chemical shifts for constitutional isomers **13** and **15**. The only difference between these two PAMs is that in **15** the ether groups are *endo*-annular while in **13** they are *exo*-annular. Apparently, the combined steric bulk of the three *endo*-annular *n*-butyl chains of the ether groups in **15** prevent the molecules from approaching each other in a face-to-face orientation.

The number of phenyl rings as well as the planar geometry of the macrocycle has a significant effect on the self-aggregation of PAMs. Even though **16**, **17**, and **18** are substituted with *n*-butyl ester groups, their K_{assoc} is diminished compared to **1** (Table 1). The smaller K_{assoc} of **17** can be attributed to the decrease in number of phenyl rings. However, the value of ΔH for **17** is much lower than the value expected if a linear relationship existed between ΔH and the number of aromatic units. The reason for this large decrease is unknown at the present time. Linear sequence **16** and PAM **18** have lower K_{assoc} than **1** even though they contain six and seven meta-linked phenylacetylene monomer units, respectively. Molecular modeling indicates that PAM **18** has a rather flexible, nonplanar geometry. Thus, the π-stacking interactions between individual aromatic rings in **18** are apparently not favored in the various conformations that this macrocycle can adopt, one of which is depicted in Figure 7.[28] This explains the decrease in self-association even though there are potentially more π-interactions per molecule in **18**. It should be noted that the van't Hoff plot for **18** was not linear between 258 and 294 K. This may suggest that **18** experiences complex conformational dynamics in this temperature range whereby different conformations may have different association constants. Analogous reasoning can be used to explain why **16**, a linear oligomer with considerable conformational flexibility, does not exhibit any solution aggregation. These observations suggest that the planar geometry of PAMs is required to bring about the π-stacking induced self-association. It can be reasoned that the well-defined, rigidly-held, planar geometry of hexameric PAMs promotes cooperative π-interactions among several pairs of aromatic rings in neigh-

(24) For a similar example see Sanders, G. M.; van Dijk, M.; van Veldhuizen, A.; van der Plas, H. C.; Hofstra, U.; Schaafsma, T. J. *J. Org. Chem.* **1988**, *53*, 5272.

(25) For a study on the influence of various solvents on dimerization of cyclophanes, see: (a) Bryant, J. A.; Knobler, C. B.; Cram, D. J. *J. Am. Chem. Soc.* **1990**, *112*, 1254. (b) Bryant, J. A.; Ericson, J. L.; Cram, D. J. *J. Am. Chem. Soc.* **1990**, *112*, 1256.

(26) This finding is consistent with the study of a series of doubly substituted 1,8-diarylnaphthalenes in which it was found that electron withdrawing groups on the aromatic rings cause a higher barrier of rotation as a result of "less unfavorable" electrostatic interaction in the ground state. See: (a) Cozzi, F.; Ponzini, F.; Annuziata, R.; Cinquini, M.; Siegel, J. S. *Angew. Chem., Int. Ed. Engl.* **1995**, *34*, 1019. (b) Cozzi, F.; Annuziata, R.; Cinquini, M.; Siegel, J. S. *J. Am. Chem. Soc.* **1993**, *115*, 5330.

(27) Exner, O. In *Correlation Analysis in Chemistry: Recent Advances*; Chapman, N. B., Shorter, J., Ed.; Plenum, New York, 1978; p 439.

(28) Molecular modeling was done using QUANTA Version 4.0, Molecular Simulations, Inc.: Waltham, MA 02154.

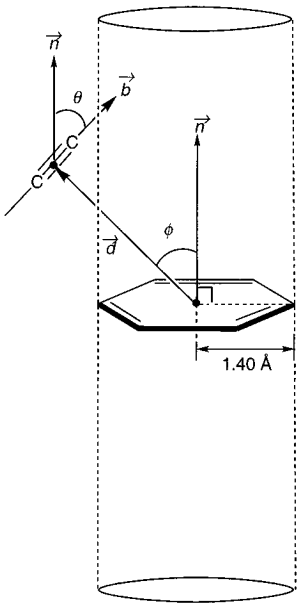

Figure 8. Geometric parameters describing the spatial relationship between acetylenic and aromatic moieties. The tilt angle (θ) and the azimuthal angle (ϕ) are indicated.

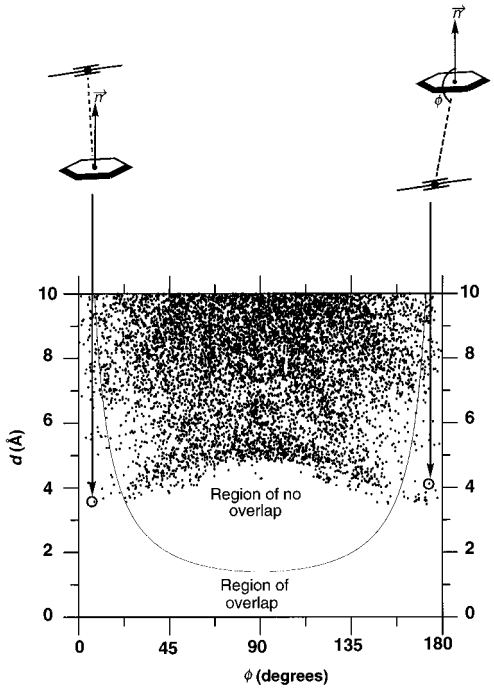

Figure 9. Plot of d vs azimuthal angle (ϕ) for the crystal structures obtained from the CSD search. The area below the solid curve defines the region where the carbon−carbon triple bond is projected within the perimeter of an aromatic ring.

boring molecules without suffering a significant reduction in conformational entropy. In other words, the individual phenyl rings of a PAM molecule are preorganized[5b] to achieve multiple $\pi-\pi$ interactions. Consequently, weak interactions between a single pair of aromatic rings that may be difficult to observe in small molecules are multiplied by the PAM molecular architecture.

What $\pi-\pi$ Interactions Drive PAM Aggregation?

Aromatic−Acetylene $\pi-\pi$ Interactions. Up to this point, the discussion has considered only aromatic−aromatic $\pi-\pi$ interactions. In contrast to the wealth of information about aromatic−aromatic interactions, much less is known about the interactions between aromatic and acetylene moieties. Due to the lack of such information, we consider here the possibility that acetylene−arene or acetylene−acetylene $\pi-\pi$ interactions may provide the driving force for the observed PAM aggregation. In order to gain insight into these interactions, the Cambridge Structural Database (CSD, Version 5.08)[29] was surveyed for structures in which the distance, d, between an aromatic centroid and the center of the carbon−carbon triple bond lies within 10 Å (Figure 8). The observed spatial distribution of triple bonds relative to the plane of the aromatic ring was compared against a random distribution to identify energetically significant interactions. Spatial overlap between an aromatic ring and a triple bond was analyzed by considering those triple bonds whose projection onto the aromatic plane fell within the phenyl ring perimeter. This information is presented in Figure 9 where d is plotted against azimuthal angle ϕ. The region that lies below the solid line is defined by the relationship given in eq 2

$$d = \frac{1.40\ \text{Å}}{\sin\phi} \qquad (2)$$

which represents the regime where the center of the carbon−carbon triple bond is projected within the aromatic perimeter (i.e., the center of the triple bond lies within a cylinder centered on an aromatic ring and of radius 1.40 Å). The CSD survey identified 293 structures and in these there were 7711 interactions between the aromatic and acetylenic moieties. Of these only 27 structures (34 interactions) lie in the overlap region as shown in Figure 9. This is lower than the value that would be expected for a random distribution of points in space (i.e., a cylinder of radius 1.40 Å and height 10.0 Å consists of ca. 1.6% of the volume of a sphere of radius 10.0 Å).[30] Close inspection of the crystal structures in the overlap region revealed that there was no correlation between the type of aromatic substituents and the occurrence of overlap.

The orientation of the triple bond with respect to the plane of the aromatic ring may also be used as an indicator of acetylene−arene $\pi-\pi$ interactions. Maximum $\pi-\pi$ interactions should occur when the mean tilt angle (θ) is 90°, i.e., the triple bond lies parallel to the aromatic plane. However, the mean tilt angle (θ) for the structures in both the overlap and nonoverlap region is ca. 90°. This leads to the conclusion that the orientation of the two moieties is statistically constant over all space. Finally, the mean value of d for structures falling within the overlap region is 3.82 Å which is somewhat smaller than for those outside the overlap region (4.68 Å). This difference, however, is likely due to the ability of a triple bond above the aromatic ring (i.e., when they are in the region of overlap) to achieve a closer approach. Substituents on the ring's perimeter prevent a similar close approach outside the overlap region. We conclude that $\pi-\pi$ stacking between triple bonds and aromatic rings is not a particularly significant noncovalent interaction.

Acetylene−Acetylene $\pi-\pi$ Interactions. $\pi-\pi$ interactions between a pair of acetylene moieties was also considered as a possible driving force for PAM aggregation. To gain insight into this interaction, the CSD was surveyed for structures in which the distance, x, between centers of carbon−carbon triple bonds was within 7 Å (Figure 10). Spatial overlap between acetylenic moieties was analyzed by considering those triple bonds whose center could be projected between the carbon

(29) Allen, F. H.; Kennard, O. *Chem. Design Automation News* **1993**, 31.

(30) For a detailed analysis of the spatial distribution of aromatic−acetylene groups and a comparision to the random spatial distribution, see the supporting information.

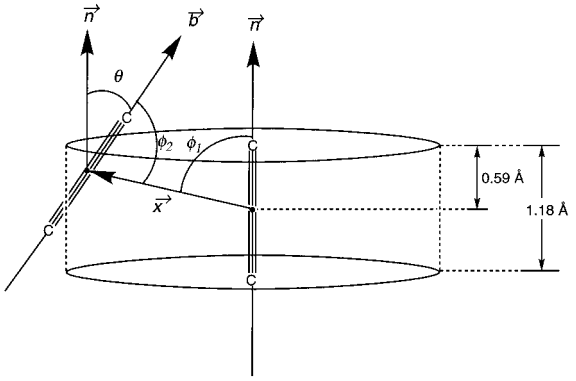

Figure 10. Geometric parameters describing the spatial relationship between two acetylenic moieties.

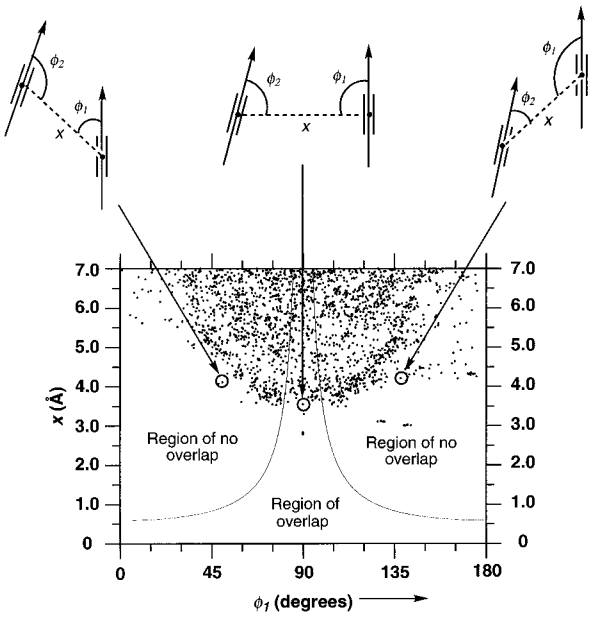

Figure 11. Plot of x vs angle ϕ_1 for the crystal structures obtained from the CSD search. The area below the solid curve defines the region where the center of one carbon−carbon triple bond is projected within the π-cylinder of the other.

atoms of another. This information is presented in Figure 11 where x is plotted against ϕ_1 (this plot is very similar to a plot of d vs ϕ_2). The solid line divides the overlap and nonoverlap regions of the centroid of one triple bond with the π-cylinder of the other as defined by eq 3

$$x = \frac{0.59\ \text{Å}}{\cos \phi_i} \quad i = 1 \text{ or } 2 \tag{3}$$

The value of 0.59 Å corresponds to half the length of a carbon−carbon triple bond. The CSD search identified 467 structures and 2105 acetylene pairs with separation distances less than 7 Å. Of these, 204 structures (349 acetylene pairs) lie in the overlap region as shown in Figure 11. A comparison of the spatial distribution of all data relative to a random distribution indicates almost no difference (see supporting information).

The orientation of one triple bond with respect to the other may also be used as an indicator of acetylene−acetylene $\pi-\pi$ interactions. Favorable association should occur when the mean tilt angle (θ) is 0° (or 180°), i.e., the triple bonds are parallel. However, the mean tilt angle (θ) for the structures in both the overlap and nonoverlap region is very near 0° (or 180°). This leads to the conclusion that the orientation of the two moieties is statistically constant regardless of position. These observations lead to the conclusion that $\pi-\pi$ stacking between triple bonds is not a particularly significant interaction.

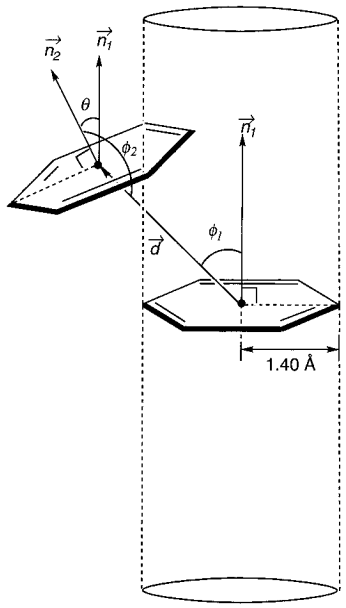

Figure 12. Geometric parameters describing the spatial relationship between a pair of aromatic moieties. The tilt angle (θ) and the azimuthal angles (ϕ_1 and ϕ_2) are indicated.

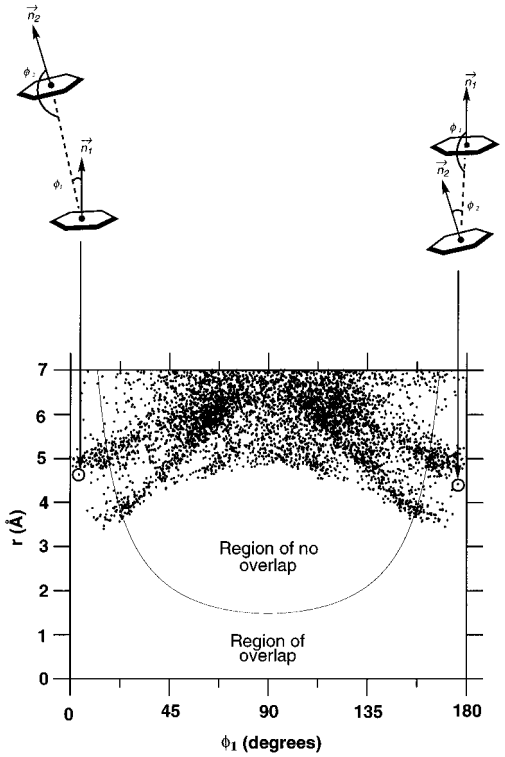

Figure 13. Plot of d vs azimuthal angle (ϕ_1) for the crystal structures obtained from the CSD search. The area below the solid curve defines the region where one aromatic ring is projected within the perimeter of the other.

To compare these π-stacking interactions to aromatic−aromatic interactions, the CSD was surveyed for structures in which the distance d, between the centroids of two aromatic rings, was within 7 Å (Figure 12). Spatial overlap between a pair of aromatic rings was analyzed by considering those aromatic rings whose projection onto the aromatic plane fell within the perimeter of the other. This information is presented in Figure 13 where d is plotted against the azimuthal angle ϕ_1 (this plot is very similar to a plot of d vs ϕ_2). The region that lies below the solid line defined using eq 2 is the regime where the centroid of one aromatic ring is projected within the perimeter of the other. The CSD survey identified 9425

structures and in these there were 48845 centroid pairs separated by less than 7 Å. Only the first ca. 10% of these data are plotted in Figure 13. The plot shows the appearance of clusters of data points indicating qualitatively significant differences in appearance from Figures 9 and 11. The spatial distribution of aromatic groups was compared to the random spatial distribution. This comparison indicated that the observed data deviated significantly from a random arrangement. In particular, there is an excess of contacts in the overlap region (see supporting information). Hence, these observations concur with the assumption that aromatic−aromatic π interactions are energetically favorable. From our analysis of the three types of pairwise interactions we conclude that the aggregation of PAMs in solution is most likely driven by $\pi-\pi$ interactions between aromatic units rather than that between aromatic−acetylene or acetylene−acetylene units.

On the nature of the Aromatic−Aromatic π-Stacking Induced Association of PAMs. In the light of these observations, we consider here the nature of π-π interactions that favor association of the PAMs. As mentioned in the introduction, various models have been proposed to address the role of molecular geometry[4a,8] and electrostatic factors[7g,9−11] in promoting aromatic association. Dipole−dipole and dipole−quadrupole interaction terms may be important for unsymmetrical molecules. However, such terms do not explain the behavior of symmetrical molecules such as PAM **1**. Association of symmetrical molecules could be explained in terms of the quadrupole−quadrupole interactions. The quadrupole−quadrupole energetic expression for a pair of aromatic rings in a face-to-face orientation, first proposed by Brown and Swinton[11b] and later modified by Hernández-Trujillo *et al.*,[11c] however, reveals that this interaction will always be repulsive for *self-association* (i.e., since self-association involves molecules with quadrupole moments of identical sign and magnitude). Thus, quadrupole−quadrupole interactions cannot favorably contribute to the stability of self-associating aromatic rings in a face-to-face geometry. It may be more useful however, to consider quadrupole−quadrupole interactions in terms of their destabilizing rather than stabilizing contribution to the overall energy. In fact, minimization of quadrupole−quadrupole repulsion in the face-to-face geometry may be one of the most significant factors that controls self-association of π-stacked aromatics. Considering quadrupole−quadrupole repulsion only, self-association would be most favored when the quadrupole moment approaches zero. Quadrupole moments of zero magnitude would occur for aromatic rings appended with the proper balance of electron withdrawing groups. These considerations suggest that the driving force for self-association may come from van der Waals interactions, which would be maximized by maximizing aromatic−aromatic contact, consistent with the face-to-face geometry. Thus, aromatic systems substituted so as to render their quadrupole moment near zero, should have the greatest propensity for self-associating in the face-to-face geometry. We recognize that this analysis is oversimplified since solvation has been ignored. Even so, its consideration will not change the fact that quadrupole−quadrupole energy of self-association in the face-to-face orientation is minimized by a quadrupole moment of zero.

Conclusions

Aromatic $\pi-\pi$ interactions induce the self-association of certain phenylacetylene macrocycles as revealed by ^{1}H NMR and VPO. The electronic character and orientation of the substituents on the PAMs strongly influences the self-associating tendency. As opposed to electron donating alkoxy or alkanoate groups, electron withdrawing ester group favor aggregation. When macrocycles have ester and alkoxy groups in the same molecule, the donor and acceptor interactions between these two groups does not promote strong aggregation. The type of alkyl group on the ester or ether derivatives is less important as long as the group is not branched and is *exo*-annular. *Endo*-annular alkyl groups as well as branched alkyl groups severely disrupt aggregation. The geometry and the size of the PAMs also influence the π-stacking interaction. A planar and rigid framework enhances the interaction while a flexible nonplanar geometry inhibits it. These observations imply that the geometry of the PAM dimer in solution involves face-to-face π-stacking. A simple model to explain this behavior is one based on minimization of quadrupole−quadrupole repulsion. Thus, face-to-face π-stacking in self-associating systems is more favorable for aromatic molecules which have a quadrupole moment near zero. Further understanding of aromatic interactions will improve our ability to control supramolecular organization, an important consideration in the rational design of condensed phases such as columnar liquid crystals, monolayer films, and crystalline solids.

Experimental Section

General Methods. The syntheses of the all macrocycles, except **6** and **15**, have been previously reported.[17] Characterization data for **6** and **15** are given in the supporting information. All compounds give satisfactory ^{1}H NMR, ^{13}C NMR, mass, and elemental analyses. Variable temperature ^{1}H NMR was done on a Bruker AM-360 equipped with a Eurotherm temperature controller and a Varian Unity 400. The temperature was calibrated with 4% methanol in methanol-d_4. All NMR spectra were taken in $CDCl_3$ with residual solvent peak as the reference. $CDCl_3$ was assumed to expand linearly with temperature and have the same expansion coefficient as $CHCl_3$.[31] The curve fitting of ^{1}H chemical shift was performed on a Macintosh personal computer using a BASIC program. Vapor pressure osmometry (VPO) was carried out on a KNAUER vapor pressure osmometer with benzil as the calibration standard in $CHCl_3$ at 308 K.

Appendix

^{1}H NMR Data Analysis. The method described below is based on that developed by Horman and Dreux.[32] For the dimerization of M, the following equilibrium is assumed

$$2\mathrm{M} \overset{K_{\mathrm{assoc}}}{\rightleftharpoons} \mathrm{M}_2 \tag{4}$$

for which, the association constant, K_{assoc}, and the total concentration (c) of the monomer are related by the following expression

$$\frac{1}{2cK_{\mathrm{assoc}}} = \frac{2[\mathrm{M}_2]}{c} + \frac{c}{2[\mathrm{M}_2]} - 2 \tag{5}$$

This equation is of the form

$$y = x + {}^1/_x - 2 \tag{6}$$

where $x = 2[\mathrm{M}_2]/c$, $y = {}^1/_2 cK_{\mathrm{assoc}}$. The parameter x thus represents the fraction of the species present as dimer. The value of x for which $0 < x < 1$ is given by

$$x = (1 = {}^y/_2) - \sqrt{(1 + {}^y/_2)^2 - 1} \tag{7}$$

If it is assumed that the measured chemical shift is the weighted average that of the monomer and dimer, then

(31) *International Critical Tables of Numerical Data: Physics, Chemistry and Technology*; Washburn, E. W., Ed.; McGraw-Hill, New York, 1928; Vol. III, p 27.

(32) Horman, I.; Dreux, B. *Helv. Chim. Acta* **1984**, *67*, 754.

$$\delta_i = \delta_0 - x(\delta_0 - \delta_d) \quad (8)$$

where δ_i is the measured chemical shift at concentration c_i, while δ_0 and δ_d are limiting chemical shifts of monomer and dimer, respectively. Equation 8 is a straight line relating δ_i to x with a slope of $-(\delta_0-\delta_d)$ and an intercept of δ_0.

In the treatment of the experimental NMR data, one first assumes a K_{assoc} value, calculates x using eq 6, and then performs linear regression calculations according to eq 8. For the line obtained, the standard deviation s of the experimental chemical shifts (δ_i) is calculated according to eq 9

$$s = \sqrt{\frac{\sum_{i=1}^{N}(\delta - \delta_i)^2}{N-1}} \quad (9)$$

where N is the number of data points, and δ is the chemical shift obtained from the linear regression. For each value of K_{assoc}, this linear regression gives values for δ_0, $\delta_0-\delta_d$, and thus, δ_d. A large standard deviation indicates that the assumed K_{assoc} is far from the correct value. Hence, in order to obtain the most accurate value for K_{assoc}, it is necessary to vary K_{assoc} over a large range which in this case varied from 10^{-4} to 10^4 of the best obtained K_{assoc} value. Therefore, unlike the Benesi−Hildebrand[33] or Wilcox−Cowart[34] methods, the Horman−Dreux method does not require the pre-estimation or extrapolation of the limiting chemical shift of monomer (δ_0) or dimer (δ_d).

The curve fitting procedure used here is justified by the following observations: (1) The association constants obtained independently from the curve fitting of different aromatic protons within the same molecule are consistent. For PAM **1**, the room temperature K_{assoc} in $CDCl_3$ obtained from chemical shifts of the *exo* aromatic proton is 62 M^{-1} while that obtained from the *endo* proton is 57 M^{-1}. (2) δ_0, obtained from the fitting, is nearly identical to that obtained from the acyclic sequence **16** which behaves as a monomer in solution. (3) δ_0 and δ_d remain essentially constant over a wide temperature range although K_{assoc} changes dramatically over the same range (see supporting information). (4) There is a good agreement between experimental data and the data obtained from the curve fitting.

VPO Data Analysis. The dimerization constant (K_2) for PAM **1** was obtained by applying the method developed by Sugawara and co-workers to the VPO data and is briefly described below.[35] In the VPO measurements, the experimentally desired osmotic coefficient ϕ,[36,37] is related to the activity coefficient (γ) using the Gibbs−Duhem equation[38]

$$\ln \gamma = (\phi - 1) + \int_0^{m_s} \frac{(\phi - 1)}{m_s} dm_s \quad (10)$$

where

$$\phi = \frac{m_c}{m_s}$$

and

$$\gamma = \frac{m_1}{m_s}$$

In the above equations, m_1 is the molal concentration of free monomer, m_s is the stoichiometric molal concentration, and m_c is the colligative molal concentration. A series expansion of eq 10 gives the dimerization constant, K_2, and higher order association constants as follows

$$\frac{m_s}{m_1} - 1 = 2K_2 m_1 + 3K_3(m_1)^2 + 4K_4(m_1)^3 + \ldots \quad (11)$$

To determine the association constants, m_c and m_s are first fitted into the following polynomial expansion

$$m_{c(\text{fitted})} = \sum_n c_n m_s^n \quad (12)$$

For PAM **1**, a fourth order polynomial gives a good fit of the experimental data as indicated in eq 13

$$m_{c(\text{fitted})} = 1.10098 m_s - 0.100638 m_s^2 + 0.00399 m_s^4 \quad (13)$$

Next γ is obtained by numerically evaluating eq 10 using the $m_{c(\text{fitted})}$ expression which affords m_1 as a function of m_s. Finally, $m_s/m_1 - 1$ was fitted to a polynomial of m_1 yielding the following empirical relationship

$$\frac{m_s}{m_1} - 1 = 0.114 m_1 - 0.0141(m_1)^2 + 0.00399(m_1)^3 \quad (14)$$

Comparison of eq 14 with eq 11 gives the values of the association constants as follows: $K_2 = 0.057$ $(\text{mm})^{-1} = 57$ M^{-1} ≈ 40 M^{-1}, and $K_3 \approx 0.0$, $K_4 \approx 0.0$. The dimerization constant (K_2) is consistent with the value of K_{assoc} obtained from the ^1H NMR study which is ca. 35 M^{-1} at 308 K in $CDCl_3$.

Acknowledgment. This work was supported by the National Science Foundation Young Investigator Program (Grant CHE-94-96105) and in part by the Petroleum Research Fund. Additional support from the 3M Company and the Camille Dreyfus Teacher−Scholar Awards Program is grateful acknowledged.

Supporting Information Available: Variable temperature ^1H NMR data, VPO measurements of the PAMs, Saunder−Hyne, error analysis on the curve fitting of the ^1H NMR data, investigation of other possible $\pi-\pi$ interactions driving PAM aggregation, ^1H NMR, ^{13}C NMR, mass spectroscopic data, and elemental analyses of PAMs **6** and **15** (55 pages). This material is contained in many libraries on microfiche, immediately follows this article in the microfilm version of the journal, can be ordered from the ACS, and can be downloaded from the Internet; see any current masthead page for ordering information and Internet access instructions.

JA9528893

(33) Benesi, H. A.; Hildebrand, J. H. *J. Am. Chem. Soc*. **1949**, *71*, 2703.
(34) Wilcox, C. S.; Cowart, M. D. *Tetrahedron Lett.* **1986**, *27*, 5563.
(35) Sugawara, N.; Stevens, E. S.; Bonora, G. M.; Toniolo, C. *J. Am. Chem. Soc*. **1980**, *102*, 7044.
(36) Robison, R. A.; Stokes, R. H. *Electrolyte Solutions*; Academic Press: New York; 1959.
(37) Glasstone, S. *Thermodynamics for Chemists*; Van Nostrand: Princeton, NJ, 1947; pp 388−392.
(38) Lewis, G. N.; Randall, M.; Pitzer, K. S.; Brewer, L. *Thermodynamics*, 2nd ed.; McGraw-Hill: New York, 1961.